Supplementary Information

An intermolecular G-quadruplex as the basis for GTP recognition in the class V GTP-aptamer

Amir H. Nasiri, Jan Philip Wurm, Carina Immer, Anna Katharina Weickhmann and Jens Wöhnert

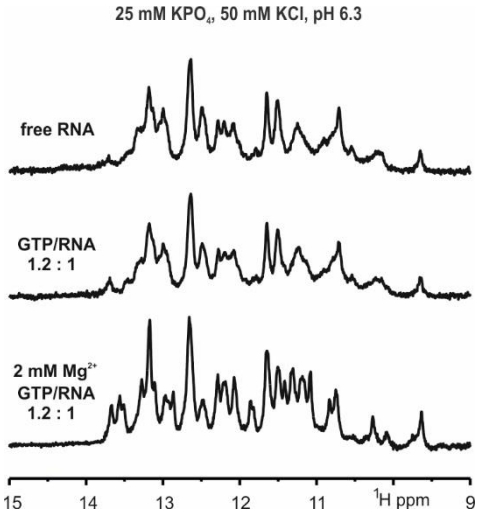

Supplementary Figure 1. GTP-binding to the class V GTP-aptamer is Mg^{2+}-dependent. Comparison of the 1D-^{1}H imino proton spectra of the RNA in the absence of both GTP and Mg^{2+} (top), in the presence of 1.2 equivalents of GTP and in the absence of Mg^{2+} (middle) and in the presence of both GTP and Mg^{2+} show that the spectral changes indicative of GTP-binding are only observable when both GTP and magnesium ions are present.

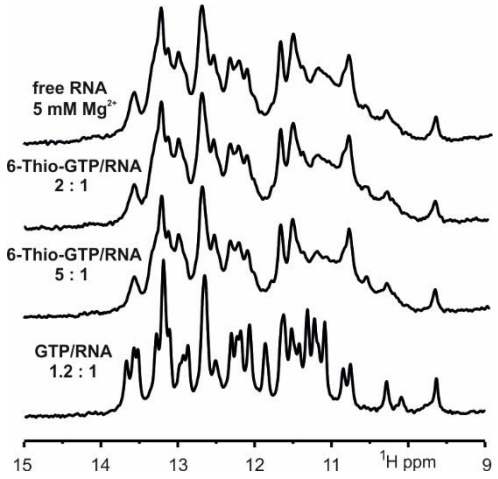

Supplementary Figure 2. 6-Thio-GTP does not bind to the class V GTP-aptamer. Comparison of the 1D-^{1}H imino proton spectra of the RNA in the presence of Mg^{2+} and in the absence of ligand (top) with spectra under the same conditions in the presence of increasing amounts of 6-Thio-GTP (middle) show that even a significant excess of 6-Thio-GTP does not induce spectral changes. The spectrum of the RNA in the presence of the binding ligand GTP and Mg^{2+} is shown at the bottom as a reference.

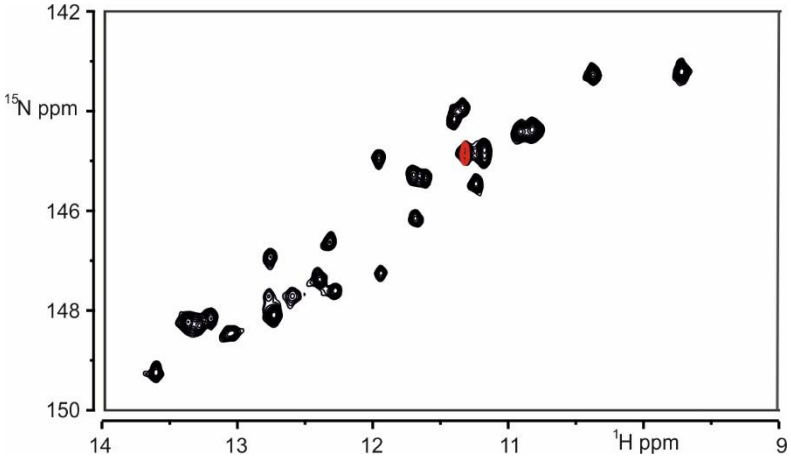

Supplementary Figure 3. Identification of the imino group resonance of the bound GTP. Shown is an overlay of the imino group regions of $^{1}H,^{15}N$-HSQC-spectra recorded for a sample of ^{15}N-guanine-labelled RNA bound to 1.2 equivalents of ^{15}N-labelled GTP (black) and for a sample containing unlabeled RNA bound to ^{15}N-labelled GTP (red). In the latter spectrum only the single signal corresponding to the imino group of the bound GTP is observable.

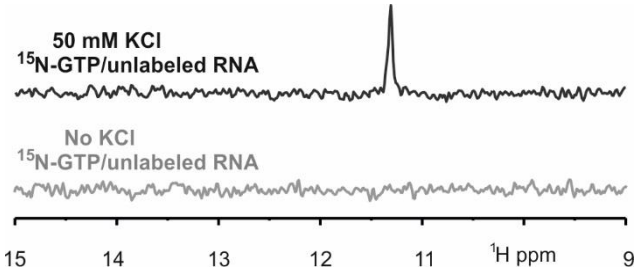

Supplementary Figure 4. GTP-binding to the class V-aptamer requires the presence of potassium ions. Shown are the 1D-slices of ^{1}H,^{15}N-HSQC-spectra recorded for samples containing unlabeled RNA and ^{15}N-labeled GTP in BisTris-buffer in the presence of 5 mM Mg^{2+} and in the absence (bottom) or presence (top) of 50 mM KCl. In the absence of KCl no imino group signal is observable indicating that GTP does not bind to the RNA under this conditions. Upon the addition of KCl the imino group signal of the bound GTP becomes visible in this experiment since now a stable complex between GTP and RNA is formed. The chemical shift for the imino proton observed in this buffer is very similar to that found in potassium phosphate buffer.

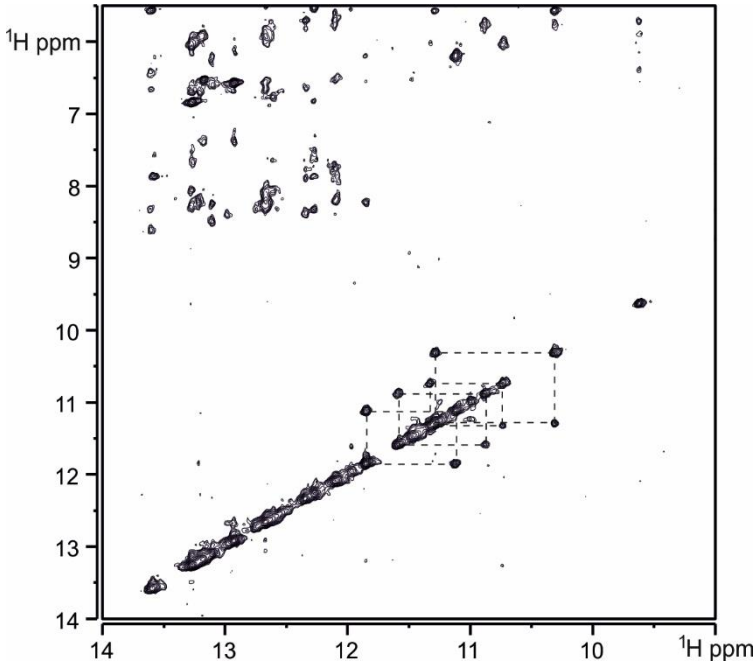

Supplementary Figure 5. ^{1}H,^{1}H-NOESY-spectrum of the free class V-aptamer in a buffer containing 25 mM $NaPO_4$, 50 mM NaCl, 2 mM $MgCl_2$, pH 6.3. The imino proton signals with chemical shifts between ~11 and 12 ppm belong to imino protons of guanine and uridine residues forming wobble G:U base pairs as indicated by their intense NOE cross peaks in agreement with the predicted secondary structure of the aptamer.

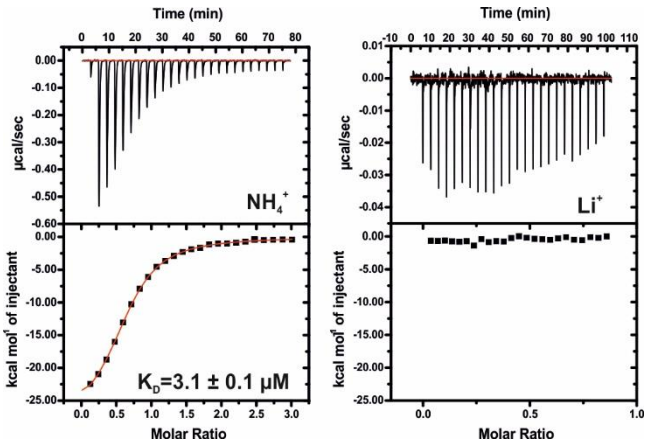

Supplementary Figure 6. GTP-binding to the class V aptamer RNA in the presence of ammonium or lithium ions. ITC thermograms and the derived binding curves for titrations of the class V aptamer with GTP in the presence of 2 mM Mg^{2+} in buffers containing either 50 mM ammonium chloride (left) or 50 mM lithium chloride (right). In the presence of ammonium ions GTP binds with a K_d of 3.1 µM whereas no binding is observed in the presence of lithium ions.

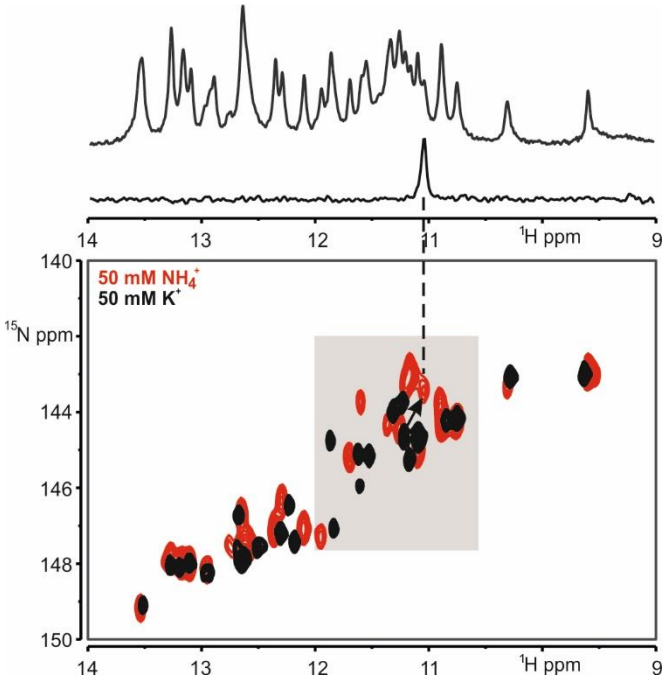

Supplementary Figure 7. GTP forms a stable 1:1 complex with the class V aptamer RNA in the presence of 50 mM ammonium chloride which is in slow exchange on the NMR time scale. (Top) Imino proton region of an 1D-^{1}H spectrum of unlabeled class V aptamer bound to unlabeled GTP in ammonium chloride containing buffer. (Middle) 1D-slice of an ^{1}H,^{15}N-HSQC-spectrum recorded in the same buffer for a sample of unlabeled RNA bound to ^{15}N-labeled GTP showing the imino group signal for the bound nucleotide. (Bottom) Overlay of 2D-^{1}H,^{15}N-HSQC-spectra of ^{15}N-guanine labeled RNA in complex with ^{15}N-labeled GTP recorded in either ammonium chloride (red) or potassium chloride (black) containing buffers. The gray box marks the chemical shift region corresponding to the guanine imino group resonances that become observable only upon GTP binding (compare to Figure 1C). An arrow indicates the chemical shift difference between the imino group resonances of the bound GTP in both buffers systems.

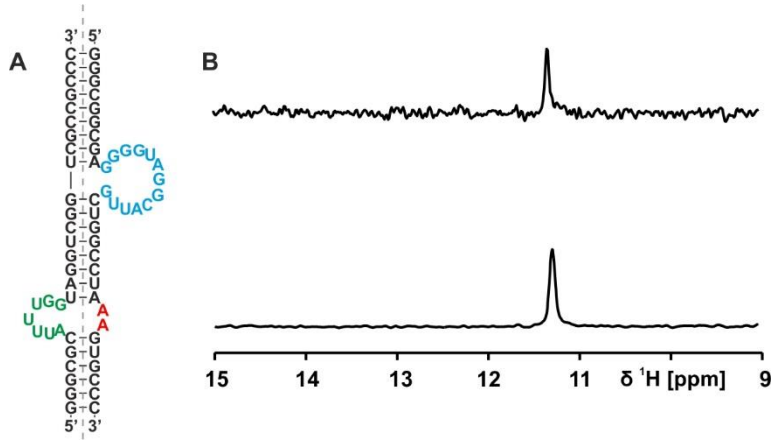

Supplementary Figure 8. GTP-binding to a mutant bipartite class V-aptamer construct containing a G61A, G62A double mutation on the 3'-side of the lower bulge. (A) Secondary structure of the mutant bipartite class V aptamer with the two G residues mutated simultaneously to A's highlighted in red. (B) Comparison of 1D-slices of $^{1}H,^{15}N$-HSQC's recorded for samples containing ^{15}N-labeled ligand GTP and unlabeled RNA for the WT-aptamer (bottom) and the double mutant bipartite construct (top). The latter spectrum was recorded at a significantly lower RNA concentration but shows a sharp imino group signal for the bound GTP at the same chemical shift as the WT in agreement with a high-affinity RNA-ligand interaction.

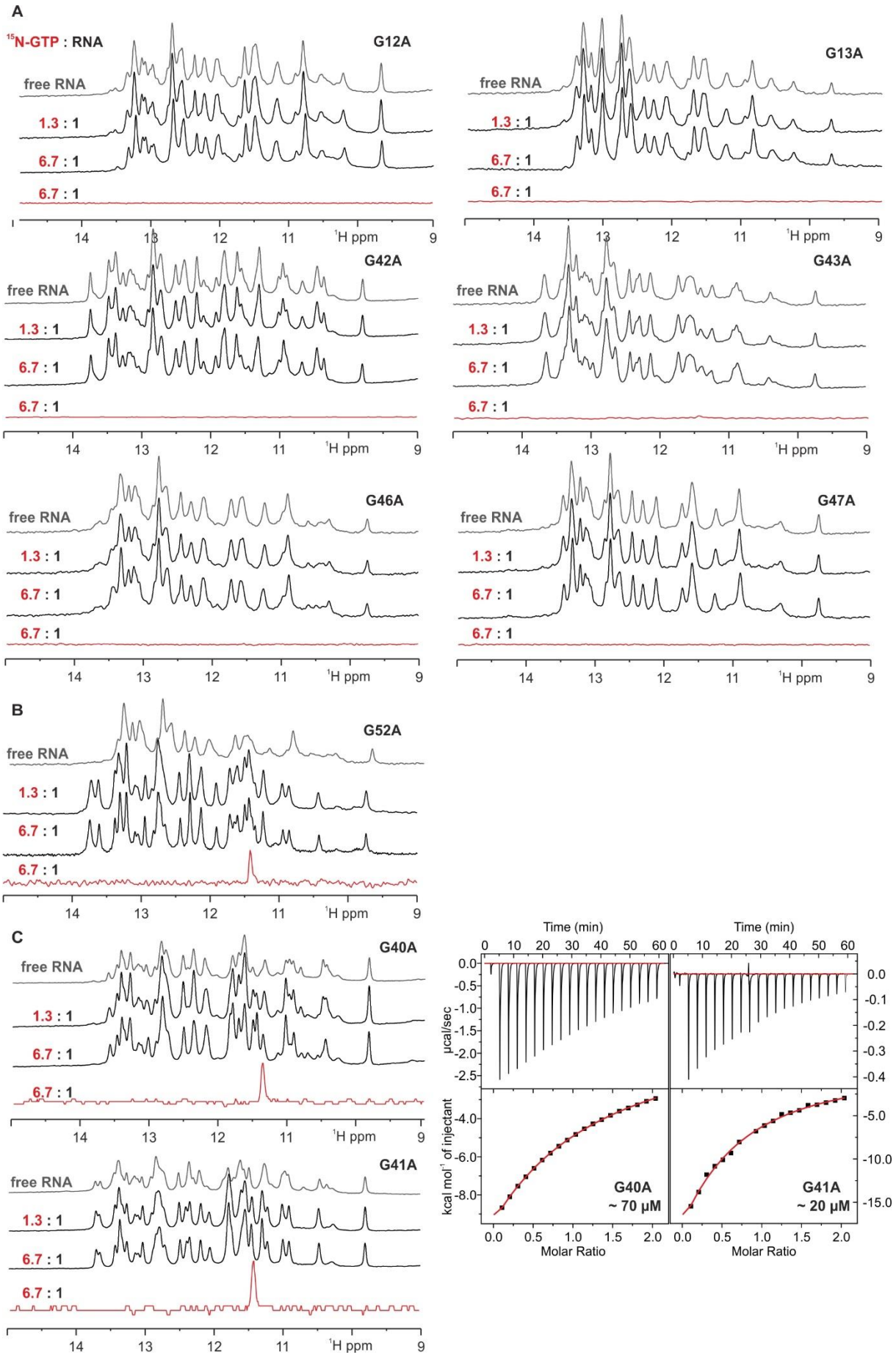
A
15N-GTP : RNA
G12A
free RNA
1.3 : 1
6.7 : 1
6.7 : 1
G13A
G42A
G43A
G46A
G47A
1H ppm
B
G52A
C
G40A
G41A
Time (min)
µcal/sec
kcal mol-1 of injectant
G40A
~ 70 µM
G41A
~ 20 µM
Molar Ratio

Supplementary Figure 9. GTP-binding to single site G to A mutants of the class V-aptamer. (A) Results of the NMR-based binding assays for the non-binding mutants G12A, G13A, G42A, G43A, G46A and G47A. Shown are comparisons of the ^{1}H-1D imino proton spectra of the free RNA (top) and in the presence of 1.3 and 6.7 equivalents of ^{15}N-labelled GTP (middle) and a 1D ^{1}H,^{15}N-HSQC-spectrum that would show the imino group signal of the bound GTP in case of binding. No changes are observed in the imino proton spectra upon addition of GTP and no signal for bound GTP is observable in the ^{1}H,^{15}N-HSQC-spectrum for these six mutants demonstrating that they lost the ability to bind GTP. (B) NMR-based binding assay for the G52A-mutant. Large spectral changes are obvious upon addition of 1.3 equivalents GTP and only very small changes occur upon addition of additional GTP. The ^{1}H,^{15}N-HSQC-spectrum (red, bottom) shows the imino group signal of the bound ^{15}N-GTP at a chemical shift similar to the WT RNA. (C) NMR-based binding assays (left) and ITC-thermograms and ITC-derived binding curves (right) for the G40A and G41A-mutants. The imino proton NMR-spectra show changes upon addition of GTP in both titration steps suggesting weaker GTP-binding compared to the WT. K_D values for both mutants were determined from ITC-experiments.

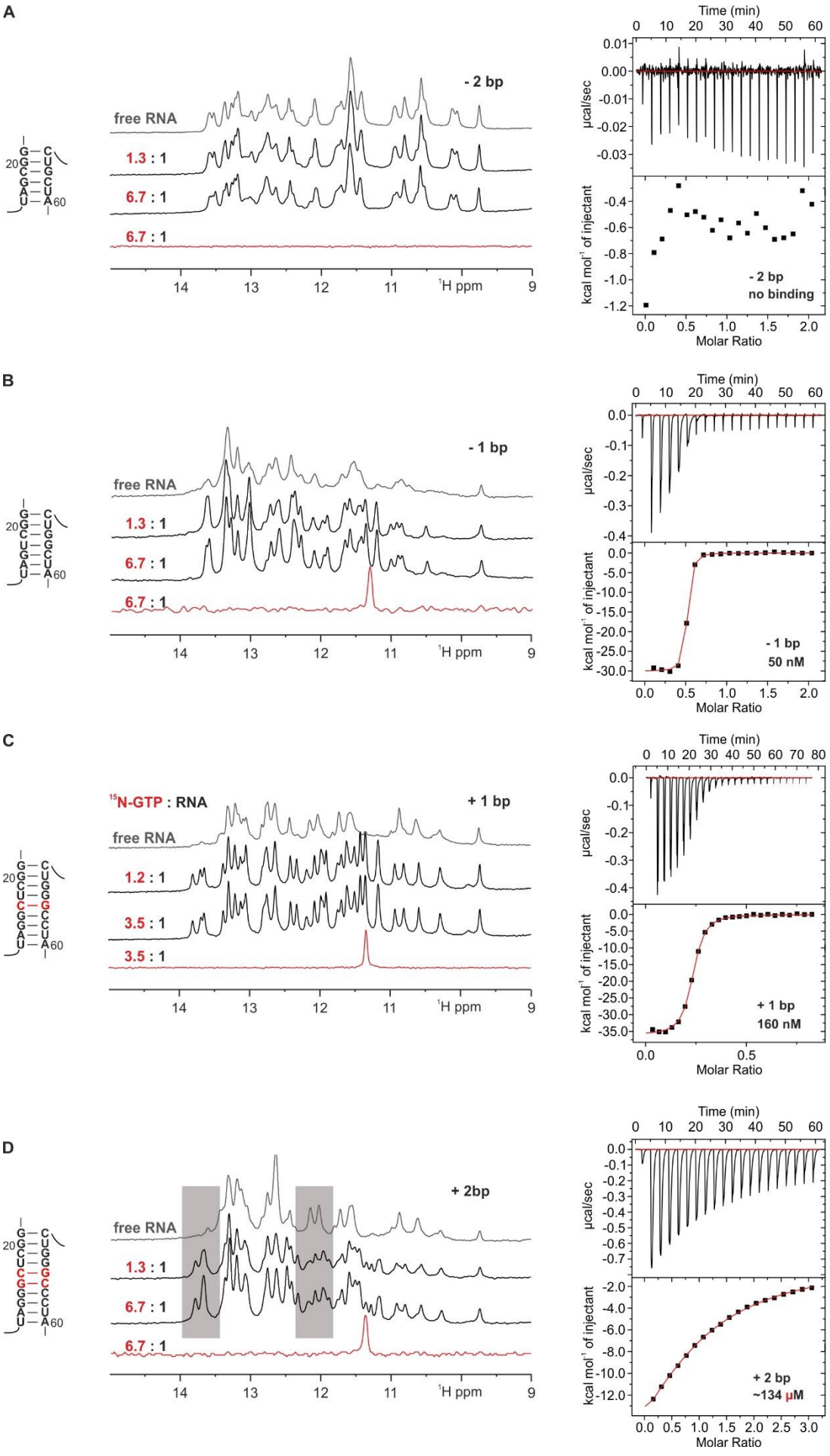
A
- 2 bp
free RNA
1.3 : 1
6.7 : 1
6.7 : 1
14 13 12 11 ¹H ppm 9
Time (min)
0 10 20 30 40 50 60
µcal/sec
kcal mol⁻¹ of injectant
- 2 bp
no binding
Molar Ratio
B
- 1 bp
free RNA
1.3 : 1
6.7 : 1
6.7 : 1
- 1 bp
50 nM
C
¹⁵N-GTP : RNA
+ 1 bp
free RNA
1.2 : 1
3.5 : 1
3.5 : 1
+ 1 bp
160 nM
D
+ 2bp
free RNA
1.3 : 1
6.7 : 1
6.7 : 1
+ 2 bp
~134 µM

Supplementary Figure 10. GTP-binding class V-aptamer constructs containing either shortened or extended variants of the central helix. In each panel (A-D) the secondary structure of the respective central helix variant is shown on the left. Additional base pairs are colored red. ^{1}H-1D imino proton spectra of the free RNA (top) and in the presence of 1.3 and 6.7 equivalents of ^{15}N-labelled GTP are shown in the middle and compared with a 1D ^{1}H,^{15}N-HSQC-spectrum showing the imino group signal of the bound GTP (bottom, red spectrum). Thermograms (top) and the derived ITC-binding curves (bottom) for each mutant are shown on the right side of each panel. (A) Aptamer variant with a two base pair deletion in the central helix. No changes in the 1D imino proton spectra of the RNA are visible upon addition of GTP and no NMR signal for the imino group of bound GTP can be observed (red spectrum). The ITC thermogram for the GTP-titration is indicative of no binding. (B) Aptamer variant with a one base pair deletion in the central helix. Significant changes of the 1D imino proton spectra compared to the free RNA are obvious upon the addition of 1.3 equivalents of GTP. No further changes occur upon addition of additional GTP. The 1D ^{1}H,^{15}N-HSQC shows the imino group of bound GTP with the same chemical shift as in the WT (red spectrum). (C) Aptamer variant with a one base pair extension in the central helix. Significant changes of the 1D imino proton spectra compared to the free RNA are already obvious upon the addition of 1.3 equivalents of GTP. No further changes occur upon addition of additional GTP. The 1D ^{1}H,^{15}N-HSQC shows the imino group of bound GTP with the same chemical shift as in the WT. (D) Aptamer variant with a two base pair extension in the central helix. Significant changes of the 1D imino proton spectra compared to the free RNA are already obvious upon the addition of 1.3 equivalents of GTP. Further changes occur upon addition of additional GTP suggesting that full saturation of binding is only reached with an excess of GTP in agreement with a lower binding affinity. Grey bars highlight those areas of the spectrum were the gradual changes upon GTp addition are easy to observe. The 1D ^{1}H,^{15}N-HSQC shows the imino group of bound GTP with a similar chemical shift as in the WT but with a larger line width. The ITC thermogram (right) shows GTP-binding with a low affinity.